DOI: 10.3901/CJME.2014.0526.300, available online at www.springerlink.com; www.cjmenet.com; www.cjmenet.com.cn

# Analytical Solutions of Cracks Emanating from an Elliptic Hole in an Infinite Plate under Tension

LIU Shuhong[1, 2, *] and DUAN Shijie[3]

1 *Department of Engineering Mechanics, Shijiazhuang Tiedao University, Shijiazhuang 050043, China*
2 *The Key Laboratory for Health Monitoring and Control of Large Structures of Hebei Province, Shijiazhuang 050043, China*
3 *Department of Adult Education, Shijiazhuang Tiedao University, Shijiazhuang 050043, China*

Received September 6, 2013; revised May 5, 2014; accepted May 26, 2014

**Abstract:** It is a common phenomenon that the cracks originating from a hole can cause structural damage in engineering. However, the fracture mechanics studies of hole edge crack problems are not sufficient. The problem of an elliptical hole with two collinear edge cracks of unequal length in an infinite plate under uniform tension at infinity is investigated. Based on the complex variable method, the analytical solutions of stress functions and stress intensity factors are provided. The stress distribution along the axes and the edge of the elliptical hole is given graphically. The numerical results show that there is obvious stress concentration near the hole and cracks, and the stresses tend to applied loads at distances far from the defect, which conform to Saint-Venant's principle. Hence, the stress functions are proved to be right. Under special conditions, the present configuration becomes the Griffith crack, two symmetrical cracks emanating from an elliptical hole, two cracks of unequal length emanating from a circular hole, a crack at the edge of a circular hole, or a crack emanating from an elliptical hole. Compared with available results, stress intensity factors for these special shapes of ellipses and cracks show good coincidence. The stress intensity factor for two cracks of unequal length at the edge of an elliptical hole increases with the crack length and the major-to-minor axis ratio of the elliptical hole. The stress distribution in an infinite plate containing an elliptic hole with unsymmetrical cracks is given for the first time.

**Keywords:** hole, crack, stress distribution, stress intensity factor

## 1 Introduction

The crack originating from a hole is an ancient problem in fracture mechanics. Even a small crack can lead to a dangerous situation. Consequently, it is of great importance to deal with hole-edge crack problems. BOWIE[1] first gave the solutions of a circular hole with a single edge crack and a pair of symmetrical edge cracks in a plate under uniform tension at infinity using the complex mapping technique. Because the mapping functions adopted are complicated and inaccurate, there are a number of papers analyzing stress intensity factors(SIFs) for cracks originating from a circular hole[2–9]. LAI, et al[10], studied the problem of a pair of cracks of different lengths emanating from the edge of a circular hole by a combined complex variable and least square method. ISIDA, et al[11], YAN[12], and GUO, et al[13–14], calculated the SIF for a single edge crack or a pair of symmetrical edge cracks originating from an elliptical hole in an infinite plate under tension. TWEED, et al[15–16], used integral transforms to obtain mode III SIF for cracks of unequal length at the edge of an elliptic hole in an infinite elastic solid. GUO, et al[17–18], studied the anti-plane problem of two asymmetrical edge cracks emanating from an elliptical hole in a piezoelectric material through the complex variable method. LIU, et al[19–20], and DU, et al[21], studied the plane problem of an elliptic hole or a crack in transversely isotropic piezoelectric materials subjected to different electro-mechanical loads. By the finite element method, LIU, et al[22], obtained the stress distributions in the vicinity of the hole and crack for the plane problem of a plate with a crack emanating from an elliptical hole. MIAO, et al[23], investigated the interactions of two collinear circular hole cracks in an infinite plate subjected to internal pressure by using a hybrid displacement discontinuity method.

This paper concerns with two cracks of unequal length at the edge of an elliptic hole in an infinite plate under tension by means of the complex variable method, and the analytical solutions of the stress functions and the stress intensity factor are obtained. In order to prove the correctness of results, numerical calculations are presented to graphically show stress distribution along the axes and

* Corresponding author. E-mail: liush@stdu.edu.cn
Supported by Hebei Provincial Natural Science Foundation of China(Grant No. A2011210033), and Foundation of Hebei Education Department of China(Grant No. ZH2011116)

the edge of the elliptical hole. To the best of my knowledge, the stress distribution is given for the first time. The values of the stress intensity factor are calculated for the cases of the elliptic hole with two collinear edge cracks of unequal length, and its degenerated shape, such as the cross crack, the elliptical(circular) hole with one crack or two symmetrical cracks.

## 2 Basic Equations

Muskhelishvili's method is used for stress analysis, the stress components $\sigma_x$, $\sigma_y$ and $\sigma_{xy}$ in rectangular coordinates are given, in terms of the complex potentials $\varphi_1(z)$ and $\psi_1(z)$, as follows:

$$\sigma_x+\sigma_y=4\,\mathrm{Re}\,\varphi_1'(z), \tag{1}$$

$$\sigma_y-\sigma_x+2\mathrm{i}\sigma_{xy}=2\left[\bar{z}\varphi_1''(z)+\psi_1'(z)\right], \tag{2}$$

where $z=x+\mathrm{i}y$ is the complex variable, the above bar denotes the complex conjugate, and the prime notation denotes differentiation with respect to $z$.

In order to make the boundary conditions more manageable, it is advantageous to replace the complex variable $z$ for any point in the $z$ plane by a new complex variable $\zeta=\rho\mathrm{e}^{\mathrm{i}\theta}$ in the $\zeta$ plane by a conformal transformation $z=\omega(\zeta)$. Then the stress functions $\varphi_1(z)$ and $\psi_1(z)$ will be considered as functions of the parameter $\zeta$. Thus, the new notation is introduced:

$$\begin{cases}\varphi(\zeta)=\varphi_1(z)=\varphi_1[\omega(\zeta)],\\ \psi(\zeta)=\psi_1(z)=\psi_1[\omega(\zeta)],\\ \Phi(\zeta)=\varphi_1'(z)=\varphi'(\zeta)/\omega'(\zeta),\\ \Psi(\zeta)=\psi_1'(z)=\psi'(\zeta)/\omega'(\zeta),\\ \Phi'(\zeta)=\varphi_1'(z)\omega'(\zeta).\end{cases} \tag{3}$$

Let $\sigma_\rho$ and $\sigma_\theta$ be the stress components in curvilinear coordinates, Eq. (1) can be rewritten as

$$\sigma_\theta+\sigma_\rho=4\,\mathrm{Re}\,\Phi(\zeta). \tag{4}$$

The functions $\varphi(\zeta)$ and $\psi(\zeta)$ can be written as

$$\varphi(\zeta)=\frac{1+\mu}{8\pi}(X+\mathrm{i}Y)\ln\zeta+B\omega(\zeta)+\varphi_0(\zeta), \tag{5}$$

$$\psi(\zeta)=-\frac{3-\mu}{8\pi}(X-\mathrm{i}Y)\ln\zeta+(B'+\mathrm{i}C')\omega(\zeta)+\psi_0(\zeta), \tag{6}$$

where

$$\varphi_0(\zeta)+\frac{1}{2\pi\mathrm{i}}\int\frac{\omega(\sigma)}{\overline{\omega'(\sigma)}}\frac{\overline{\varphi_0'(\sigma)}}{\sigma-\zeta}\mathrm{d}\sigma=\frac{1}{2\pi\mathrm{i}}\int\frac{f_0}{\sigma-\zeta}\mathrm{d}\sigma, \tag{7}$$

$$\psi_0(\zeta)+\frac{1}{2\pi\mathrm{i}}\int\frac{\overline{\omega(\sigma)}}{\omega'(\sigma)}\frac{\varphi_0'(\sigma)}{\sigma-\zeta}\mathrm{d}\sigma=\frac{1}{2\pi\mathrm{i}}\int\frac{\overline{f_0}}{\sigma-\zeta}\mathrm{d}\sigma, \tag{8}$$

$$f_0=\mathrm{i}\int(\overline{X}+\mathrm{i}\overline{Y})\mathrm{d}s-\frac{X+\mathrm{i}Y}{2\pi}\ln\sigma-\frac{1+\mu}{8\pi}(X-\mathrm{i}Y)\frac{\omega(\sigma)}{\overline{\omega'(\sigma)}}\sigma-2B\omega(\sigma)-(B'-\mathrm{i}C')\overline{\omega(\sigma)}, \tag{9}$$

where $\overline{X}$, $\overline{Y}$ represent the components of the surface forces per unit area at any point of the interior boundary, $X$ and $Y$ are the sums of the surface force components on the interior boundaries in the $x$ and $y$ directions. The constants $B$ and $B'+\mathrm{i}C'$ are related to the magnitudes of the principal stresses $\sigma_1$ and $\sigma_2$ at infinity, i.e.,

$$\begin{cases}B=\dfrac{1}{4}(\sigma_1+\sigma_2),\\ B'+\mathrm{i}C'=-\dfrac{1}{2}(\sigma_1-\sigma_2)\mathrm{e}^{-2\mathrm{i}\alpha},\end{cases} \tag{10}$$

where $\alpha$ is the angle made by $\sigma_1$ with $x$ axis.

## 3 Problem and Exact Solutions

Consider two collinear edge cracks of unequal length emanating from an elliptical hole in an infinite plate. The cracks and hole are assumed to be traction free while the plate is subjected to uniform remote tensile stress $q$ in the $y$ direction, as shown in Fig. 1. The rectangular coordinates system is set with the origin at the center of the elliptical hole and the $x$-axis coinciding with the line at which the cracks are located.

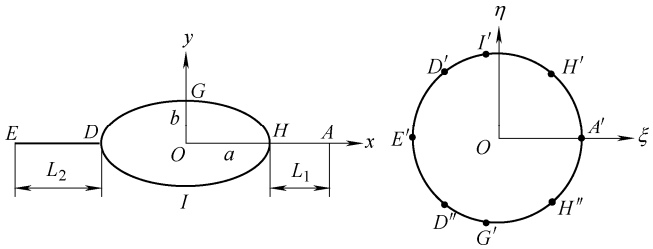


Fig. 1. Mapping the elliptical hole with two cracks of unequal length into the unit circle

### 3.1 Stress functions

The conformal mapping function(GUO, et al[17–18]) is

$$z=\omega(\zeta)=\frac{a+b}{2}\mu(\zeta)+\frac{a-b}{2}\frac{1}{\mu(\zeta)}, \tag{11}$$

where

$$\begin{cases}\mu(\zeta)=(m+n)/4\zeta,\\ m=\varepsilon_1(1+\zeta)^2+\varepsilon_2(1-\zeta)^2,\\ n=\left[\left(\varepsilon_1^2-1\right)(1+\zeta)^4+2(\varepsilon_1\varepsilon_2+1)(1-\zeta^2)^2+\right.\\ \qquad\left.(\varepsilon_2^2-1)(1-\zeta)^4\right]^{\frac{1}{2}},\end{cases} \tag{12}$$

$$\varepsilon_i=\frac{(a+L_i)^2+b^2+ab+(a+L_i)\sqrt{L_i^2+2aL_i+b^2}}{(a+b)(a+L_i+\sqrt{L_i^2+2aL_i+b^2})}\quad(i=1,\ 2).\tag{13}$$

Eq. (11) provides a conformal mapping from the outside region of the elliptical hole and cracks in the $z$ plane into the interior of a unit circle in the $\zeta$ plane, $A(a+L_1,\ 0)\rightarrow A'(1,\ 0)$, $I(0,\ -b)\rightarrow I'$, $E(-a-L_2,\ 0)\rightarrow E'(-1,\ 0)$, and $G(0,\ b)\rightarrow G'$. At the same time, the lower points $H(a,\ 0)$ and $D(-a,\ 0)$ are mapped to points $H'$ and $D'$, the upper points $H$ and $D$ to points $H''$ and $D''$.

Under the present loading condition, it can be seen that $B=q/4$, $B'+\mathrm{i}C'=q/2$, $\overline{X}=\overline{Y}=X=Y=0$. Thus Eq. (9) is simplified as

$$f_0=-\frac{q}{2}\omega(\sigma)-\frac{q}{2}\overline{\omega(\sigma)}.\tag{14}$$

From Eqs. (11)–(12), one can obtain the following equations:

$$\omega'(\zeta)=-\frac{(1-\zeta^2)(\varepsilon_1+\varepsilon_2)}{4\zeta^2}\left(\frac{bm}{\sqrt{m^2-16\zeta^2}}+a\right),\tag{15}$$

$$\omega'(\frac{1}{\zeta})=\frac{(1-\zeta^2)(\varepsilon_1+\varepsilon_2)}{4}\left(\frac{bm}{\sqrt{m^2-16\zeta^2}}+a\right).\tag{16}$$

On the unit circle, since $\overline{\sigma}=1/\sigma$, $\overline{\omega'(\sigma)}=\overline{\omega}'(\overline{\sigma})$, it can be found that $\omega(\sigma)\overline{\varphi_0'(\sigma)}/\overline{\omega'(\sigma)}$ is analytical outside the unit circle, and continuous outside and on the circle. $\overline{\omega(\sigma)}\varphi_0'(\sigma)/\omega'(\sigma)$ is analytical in the circle hole, and also continuous inside and on the circle. Then, using Cauchy integral, one can obtain

$$\frac{1}{2\pi\mathrm{i}}\int\frac{\omega(\sigma)}{\overline{\omega'(\sigma)}}\frac{\overline{\varphi_0'(\sigma)}}{\sigma-\zeta}\mathrm{d}\sigma=0.\tag{17}$$

Substituting Eqs. (14) and (17) into Eq. (7) produces

$$\varphi_0(\zeta)=\frac{1}{2\pi\mathrm{i}}\int\frac{-\frac{q}{2}\omega(\sigma)-\frac{q}{2}\overline{\omega(\sigma)}}{\sigma-\zeta}\mathrm{d}\sigma.\tag{18}$$

Clearly, both $\omega(\zeta)$ and $\overline{\omega(\zeta)}$ have two poles of the 1st order $\zeta=0$ and $\zeta=\infty$, and

$$\mathrm{Res}(\omega(\zeta),0)=\frac{(a+b)(\varepsilon_1+\varepsilon_2)}{4},\tag{19}$$

$$\mathrm{Res}(\overline{\omega(\zeta)},\infty)=-\frac{(a+b)(\varepsilon_1+\varepsilon_2)}{4},\tag{20}$$

where "Res" denotes the residue.

Substituting Eqs. (19)–(20) into Eq. (18), the following expressions can be obtained:

$$\varphi_0(\zeta)=-\frac{q}{2}\omega(\zeta)+\frac{q(a+b)(\varepsilon_1+\varepsilon_2)}{8}\left(\frac{1}{\zeta}-\zeta\right).\tag{21}$$

From Eq. (13), when $L_1=L_2=0$, $\varepsilon_1=\varepsilon_2=1$ can be obtained, the elliptic hole with two cracks of unequal length degenerates to the elliptical hole. From Eqs. (11)–(13) and (21), we have

$$\varphi_0(\zeta)=-\frac{qa}{2}\zeta.\tag{22}$$

This is just the well-known result for the elliptical hole.

Differentiating Eq. (21) with respect to $\zeta$, one can obtain

$$\varphi_0'(\zeta)=-\frac{q}{2}\omega'(\zeta)-\frac{q(a+b)(\varepsilon_1+\varepsilon_2)}{8}\left(\frac{1}{\zeta^2}+1\right).\tag{23}$$

Substituting Eqs. (14) and (21) into Eq. (8), and using Cauchy integral again, we have

$$\psi_0(\zeta)=-\bar{z}\frac{\varphi_0'(\zeta)}{\omega'(\zeta)}-q\left[\frac{1}{2}\omega(\zeta)-\frac{(a+b)(\varepsilon_1+\varepsilon_2)}{8}\left(\frac{1}{\zeta}-\zeta\right)\right].\tag{24}$$

Substituting Eqs. (10)–(11), (21), (24) into Eqs. (5)–(6) yields

$$\varphi(\zeta)=-\frac{q}{4}\omega(\zeta)+\frac{q(a+b)(\varepsilon_1+\varepsilon_2)}{8}\left(\frac{1}{\zeta}-\zeta\right),\tag{25}$$

$$\psi(\zeta)=-\bar{z}\frac{\varphi_0'(\zeta)}{\omega'(\zeta)}+\frac{(a+b)(\varepsilon_1+\varepsilon_2)}{8}\left(\frac{1}{\zeta}-\zeta\right).\tag{26}$$

Hence, substituting Eqs. (3) and (25)–(26) into Eqs. (1)–(2), the stress components $\sigma_x$, $\sigma_y$ and $\sigma_{xy}$ in terms of the complex variable $\zeta$ can be obtained. These expressions are too lengthy to be written here. At the edge of the elliptical hole, there is $\sigma_\rho=0$, then, from Eq. (4), one can obtain $\sigma_\theta=4\Phi(\zeta)$.

### 3.2 Stress intensity factors

The opening and sliding mode stress intensity factors $K_\mathrm{I}$ and $K_\mathrm{II}$ at the crack tip $A$ are defined by

$$K_\mathrm{I}+\mathrm{i}K_\mathrm{II}=2\sqrt{2\pi}\lim_{\zeta\rightarrow1}\sqrt{\omega(\zeta)-\omega(1)}\frac{\varphi'(\zeta)}{\omega'(\zeta)}=2\sqrt{\pi}\frac{\varphi'(1)}{\sqrt{\omega''(1)}}.\tag{27}$$

Inserting Eqs. (11) and (25) into Eq. (27), we have

$$K_{\mathrm{I}}=\frac{\sqrt{2\pi}q(a+b)\sqrt{\varepsilon_1+\varepsilon_2}\sqrt[4]{\varepsilon_1^2-1}}{2\sqrt{b\varepsilon_1+a\sqrt{\varepsilon_1^2-1}}}, \tag{28}$$

$$K_{\mathrm{II}}=0. \tag{29}$$

Eq. (28) shows that stress intensity factors for cracks of unequal length emanating from the edge of an elliptical hole in an infinite plate are related to the applied mechanical loading, hole size and crack length.

## 4 Numerical Results and Discussions

### 4.1 Stress distribution

In this section, in order to prove the correctness of the stress functions, numerical calculations are presented to graphically show stress distribution along the axes and the edge of the elliptical hole. Assume the dimensions of the hole and cracks as follows: $a$=2 m, $b$=1 m, $L_1$=2 m and $L_2$=1 m.

Fig. 2 shows the normalized stress distribution of $\sigma_x/q$, $\sigma_{xy}/q$ and $\sigma_y/q$ along the negative $x$ axis. The distance between the first point and the left crack tip is 0.01 m, and the range of $x$ is from −3.01 m to −12 m. It can be seen that stress $\sigma_x/q$ and $\sigma_y/q$ decrease rapidly with $x$, $\sigma_x/q$ from 11.452 to 0, and $\sigma_y/q$ from 12.452 to 1. Because of symmetry, $\sigma_{xy}/q$ is always zero. There is obvious stress concentration in the neighborhood of the crack tip.

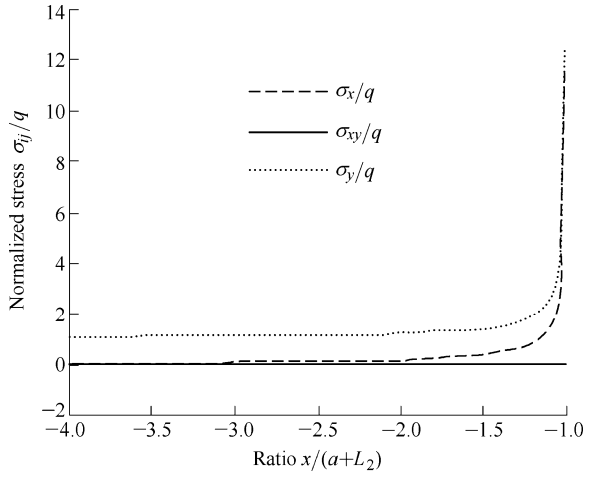


Fig. 2. Normalized stress distribution along negative axis $x$

Fig. 3 shows the normalized stress distribution of $\sigma_x/q$, $\sigma_{xy}/q$ and $\sigma_y/q$ along the $y$ axis. It can be seen that $\sigma_x/q$ increases rapidly from −1 to 0, and $\sigma_y/q$ first decreases from 0 to a negative value, then increases to 1. The shearing stress $\sigma_{xy}/q$ isn't always zero.

Fig. 4 shows the variation of the normalized stress $\sigma_\theta/q$ with $\theta$ on the half edge of the elliptical hole when $L_2$=1 m and $L_2$=0. By Eq. (11), when $L_2$=1 m, the rectangular coordinates of $D''$, $G'$ and $H''$ are −0.8614−0.5079i, −0.1062−0.9943i, and 0.6490−0.7608i, the corresponding $\theta$ are 3.6743 rad, 4.6060 rad and 5.4186 rad. When $L_2$=0, the rectangular coordinates of $D''$, $G'$ and $H''$ are −1, −0.1886−0.9821i, 0.6228−0.7824i, the corresponding $\theta$ are π rad, 4.5227 rad and 5.3848 rad. It can be seen that the stress in the tangential direction changes obviously. However, for the two different cases, $\sigma_\theta/q$=−1 at the point of $G$. The results are coincident with those in LIU, et al [22].

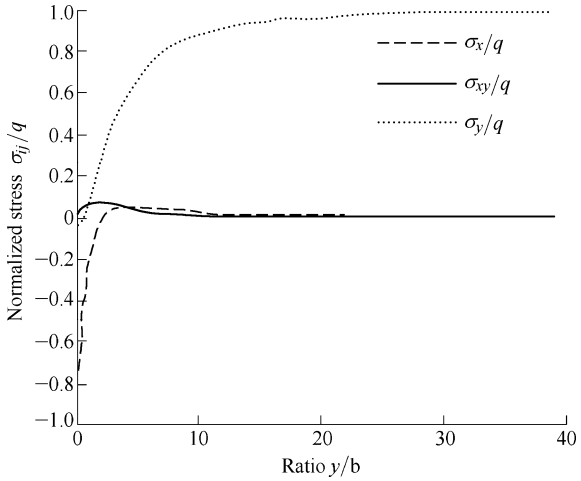


Fig. 3. Normalized stress distribution along axis $y$

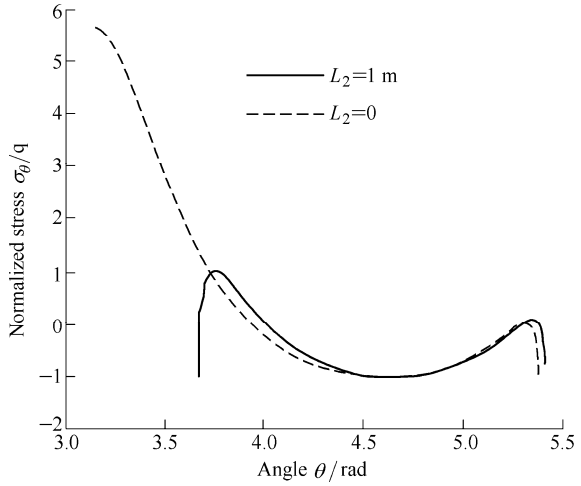


Fig. 4. Variation of normalized stress $\sigma_\theta/q$ with $\theta$

From Figs. 2−4, it can be seen that if an elliptical hole with two cracks of unequal length is made in an infinite plate, the stress distribution in the neighborhood of the hole and cracks changes significantly, but the stress distribution is practically uniform at distances which are large compared with the size of the defect. These phenomena conform to conclusions usually made on the basis of Saint-Venant's principle.

### 4.2 Stress intensity factors

Under specific conditions, some configurations discussed in the exiting literatures can be simulated from the present results, such as the Griffith crack, two symmetrical cracks emanating from an elliptical hole, two cracks of unequal length emanating from a circular hole, a crack at the edge of a circular hole, and a crack emanating from an elliptical hole. Discussion is given as follows.

If $b$=0, $L_1$=$L_2$=$L$, Eq. (28) is reduced to $K_{\mathrm{I}}=q\sqrt{\pi(a+L)}$, which is just the well-known result of the Griffith crack.

If $L_2$=$L_1$, Eq. (28) is the result of two symmetrical cracks emanating from the edge of an elliptical hole. Fig. 5 illustrates the variation of $K_{\mathrm{I}}$ with $b$ for four different crack lengths when $a$=1 m and $q$=1 Pa. It can be seen that the result agrees to the previous work(GUO, et al[14]).

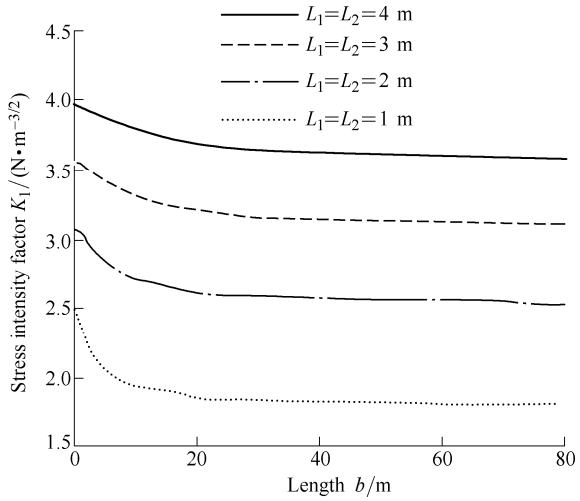


Fig. 5. Variation of $K_{\mathrm{I}}$ with $b$ for two symmetrical cracks emanating from an elliptical hole

If $a$=$b$, Eq. (28) becomes the result of two cracks of unequal length originating from a circular hole. The variation of normalized stress intensity factors $K_{\mathrm{I}}/K_0$ with $a_2/a$ for various $a_2/a_1$ is shown in Fig. 6, where $a$=$b$=1 m, $a_1$=$L_1$+$a$, $a_2$=$L_2$+$a$, and $K_0=q\sqrt{\pi a}$. In order to observe visually, the values of $K_{\mathrm{I}}/K_0$ for $a_2/a$=4 are listed in Table 1. It can be seen that Fig. 6 and Table 1 are quite similar to those previously obtained in LAI, et al[10].

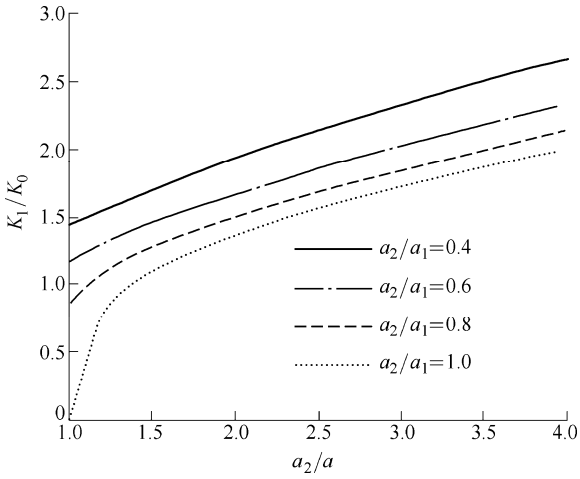


Fig. 6. Variation of $K_{\mathrm{I}}/K_0$ with $a_2/a$ for two cracks of unequal length emanating from a circular hole

If $a$=$b$, and $L_2$=0, Eq. (28) degenerates into the result of a crack at the edge of a circular hole. Fig. 7 shows the variation of the normalized stress intensity factors $K_{\mathrm{I}}/K_0$ with $L_1/b$ when $a$=$b$=1 m and $L_2$=0. The results are identical to those previously obtained in TWEED, et al[3].

**Table 1. $K_{\mathrm{I}}$ / $K_0$ for a pair of cracks emanating from a circular hole ($a_2/a$=4)**

| Ratio $a_2/a_1$ | Present $(K_1/K_0)_P$ | Ref. [10] $(K_1/K_0)_L$ | Difference $\dfrac{(K_1/K_0)_P-(K_1/K_0)_L}{(K_1/K_0)_P}\Big/\%$ |
|---|---|---|---|
| 1.0 | 1.996 1 | 2.015 3 | –0.96 |
| 0.9 | 2.057 7 | 2.066 5 | –0.43 |
| 0.8 | 2.129 8 | 2.129 8 | 0.00 |
| 0.7 | 2.216 8 | 2.209 7 | 0.32 |
| 0.6 | 2.325 7 | 2.313 0 | 0.55 |
| 0.5 | 2.468 0 | 2.451 3 | 0.68 |
| 0.4 | 2.665 2 | 2.646 3 | 0.71 |

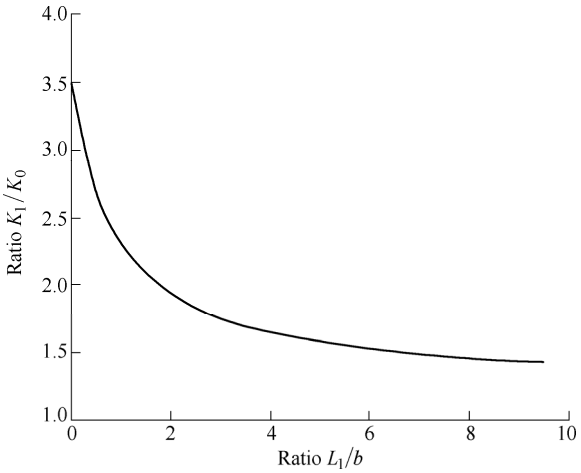


Fig. 7. Variation of $K_{\mathrm{I}}/K_0$ with $L_1/b$ for a crack at the edge of a circular hole

If $L_2$=0, Eq. (28) is simplified to the result of a single edge crack emanating from an elliptical hole. The expression of $K_{\mathrm{I}}$ is the same as that given by GUO, et al[13]. Fig. 8 illustrates the variation of $K_{\mathrm{I}}$ with $b$ for four different values of $L_1$ when $a$=1 m and $q$=1 Pa. It can be seen that as $b$ increases, the value of $K_{\mathrm{I}}$ first increases, and reaches the maximum value, then decreases to a stable value. In addition, the value of $K_{\mathrm{I}}$ also increases with $L_1$ at a given value of $b$.

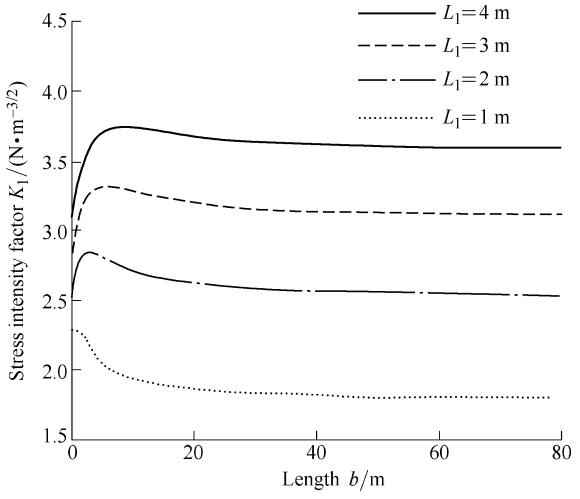


Fig. 8. Variation of $K_{\mathrm{I}}$ with $b$ for a crack emanating from an elliptical hole

Figs. 9 and 10 illustrate the variation of $K_I$ with $L_1$ for two cracks of unequal length at the edge of an elliptical hole. In Fig. 9 $L_2$=3 m, $b$=1 m and $q$=1 Pa, and $a$=5 m, $b$=1 m and $q$=1 Pa in Fig. 10. It is found that the value of $K_I$ increases as the ratio of $a/b$ and the crack length become larger.

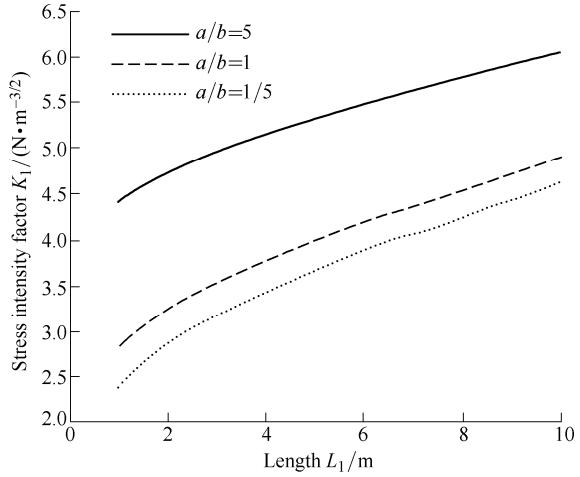


Fig. 9. Variation of $K_I$ with $L_1$ for two cracks of unequal length emanating from an elliptical hole($L_2$=3 m)

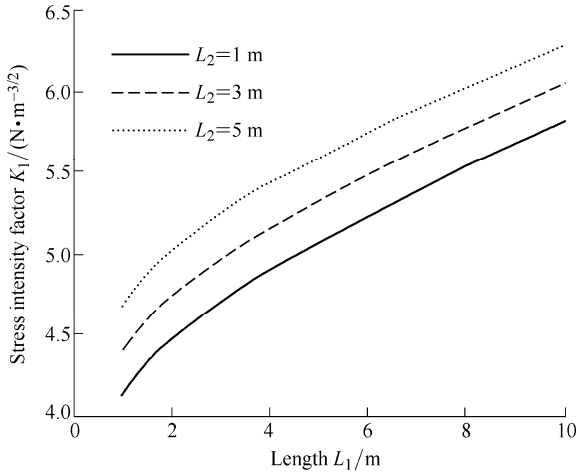


Fig. 10. Variation of $K_I$ with $L_1$ for two cracks of unequal length emanating from an elliptical hole ($a/b$=5)

If $a$=0, Eq. (28) represents the result of asymmetrical cross-shaped cracks. Especially, when $L_2$ is also equal to zero, Eq. (28) denotes the result of T-shaped cracks. Finally, the variation of $K_I$ with $b$ for the cases of asymmetrical cross-shaped cracks and T-shaped cracks are shown in Figs. 11 and 12, respectively. As shown in Fig. 11, when $L_1$= $L_2$=5 m, the value of $K_I$ is not influenced by $b$. If $L_2$ is smaller than $L_1$, it increases with $b$. On the other hand, if $L_2$ is greater than $L_1$, it decreases as $b$ increases. Furthermore, when $b$ is great enough, the value of $K_I$ for any $L_2$ is close to 3.9633 N • m$^{-3/2}$, which corresponds to the case of symmetrical cross-shaped cracks of $L_1$= $L_2$=5 m. It can be observed that the curves in Fig. 12 are similar to those in Fig. 8. The differences are that the values of $K_I$ for T-shaped cracks are smaller than those for a crack emanating from an elliptical hole when $L_1$ is the same.

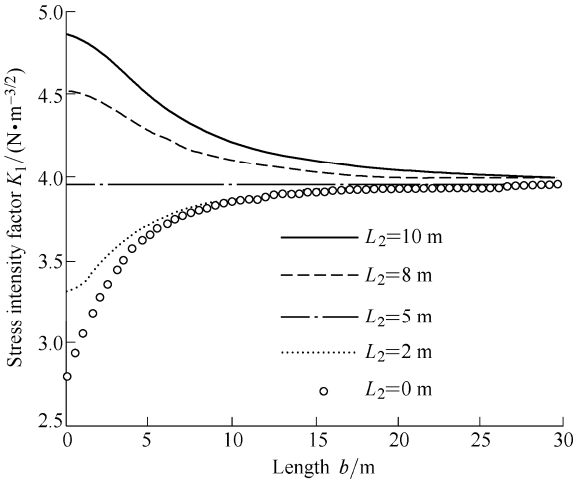


Fig. 11. Variation of $K_I$ with $b$ for asymmetrical cross-shaped cracks ($L_1$=5 m)

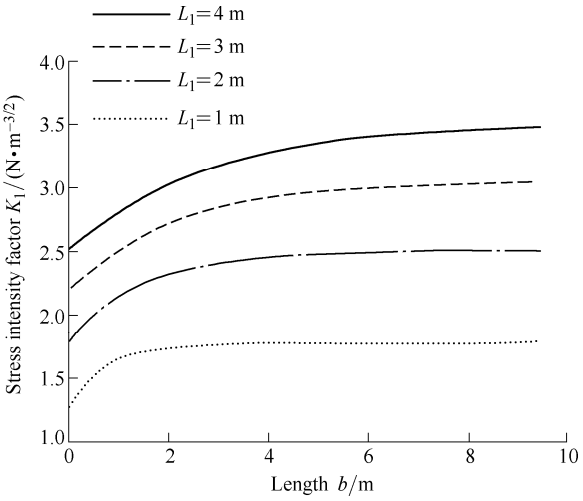


Fig. 12. Variation of $K_I$ with $b$ for T-shaped crack

## 5 Conclusions

(1) The analytical solutions of the stress functions and the stress intensity factor are derived for the problem of an elliptical hole with two cracks of unequal length in an infinite plate under remote tension.

(2) There is always a compressive stress that equals the applied tension stress at two ends of the minor axis for different elliptical shapes.

(3) The stress intensity factors for some particular hole-edge cracks are in good agreement with the existing results.

(4) The stress intensity factors increase with the crack length and the major-to-minor axis ratio of the elliptical hole.

(5) For symmetrical cross-shaped cracks, the stress intensity factor isn't influenced by the length of the semi-minor axis.

### References

[1] BOWIE O L. Analysis of an infinite plate containing radial cracks originating at the boundary of an internal circular hole[J]. *Journal of Mathematics and Physics*, 1956, 35: 60–71.

[2] TWEED J, ROOKE D P. The distribution of stress near the tip of a radial crack at the edge of a circular hole[J]. *International Journal of Engineering Science*, 1973, 11(11): 1185–1195.

[3] TWEED J, ROOKE D P. The stress intensity factor for a crack at the edge of a loaded hole[J]. *International Journal of Solids and Structures*, 1979, 15(11): 899–906.

[4] SCHIJVE J, LAI J. The stress intensity factor of hole edge cracks in a finite width plate[J]. *International Journal of Fracture*, 1990, 46(3): 37–42.

[5] SCHIJVE J. Comparison between empirical and calculated stress intensity factors of hole edge cracks[J]. *Engineering Fracture Mechanics*, 1985, 22(1): 49–58.

[6] LIN X B, SMITH R A. Stress intensity factors for corner cracks emanating from fastener holes under tension[J]. *Engineering Fracture Mechanics*, 1999, 62(6): 535–553.

[7] ABDELMOULA R, SEMANI K, LI J. Analysis of cracks originating at the boundary of a circular hole in an infinite plate by using a new conformal mapping approach[J]. *Applied Mathematics and Computation*, 2007, 188(2): 1891–1896.

[8] STEFANESCU D, EDWARDS L, FITZPATRICK M E. Stress intensity factor correction for asymmetric through-thickness fatigue cracks at holes[J]. *International Journal of Fatigue*, 2003, 25(7): 569–576.

[9] ZHAO J F, XIE L Y, LIU J Z, et al. A method for stress intensity factor calculation of infinite plate containing multiple hole-edge cracks[J]. *International Journal of Fatigue*, 2012, 35(1): 2–9.

[10] LAI J B, ZHANG X, SCHIJVE J. An investigation of a hole-edge crack problem by a combined complex variable and least square method[J]. *Engineering Fracture Mechanics*, 1991, 39(4): 713–737.

[11] ISIDA M, CHEN D H, NISITANI H. Plane problems of an arbitrary array of cracks emanating from the edge of an elliptical hole[J]. *Engineering Fracture Mechanics*, 1985, 21(5): 983–995.

[12] YAN X Q. A numerical analysis of cracks emanating from an elliptical hole in a 2-D elasticity plate[J]. *European Journal of Mechanics. A: Solids*, 2006, 25(1): 142–153.

[13] GUO H M, LIU G T, PI J D. Stress analysis of an ellipse hole with a straight edge-crack by complex variable method[J]. *Acta Mechanica Solida Sinica*, 2007, 28(3): 308–312. (in Chinese)

[14] GUO J H, LIU G T. Stress analysis for an elliptical hole with two straight cracks[J]. *Chinese Journal of Theoretical and Applied Mechanics*, 2007, 39(5): 699–703. (in Chinese)

[15] TWEED J, MELROSE G. Cracks of unequal length at the edge of an elliptic hole in out of plane shear[J]. *Applied Mathematics Letters*, 1989, 2(2): 171–174

[16] TWEED J, MELROSE G. Cracks at the edge of an elliptic hole in out of plane shear[J]. *Engineering Fracture Mechanics*, 1989, 34(3): 743–747.

[17] GUO J H, LU Z X, HAN H T, et al. The behavior of two non-symmetrical permeable cracks emanating from an elliptical hole in a piezoelectric solid[J]. *European Journal of Mechanics. A: Solids*, 2010, 29(4): 654–663.

[18] GUO J H, LU Z X, HAN H T, et al. Exact solutions for anti-plane problem of two asymmetrical edge cracks emanating from an elliptical hole in a piezoelectric material[J]. *International Journal of Solids and Structures,* 2009, 46(21): 3799–3809

[19] LIU S H, SHEN Y M, LIU J X. Exact solutions for piezoelectric materials with an elliptic hole or a crack under uniform internal pressure[J]. *Chinese Journal of Mechanical Engineering*, 2012, 25(4): 845–852.

[20] LIU S H, LI Y Q, SHEN Y M. The electro-elastic fields of piezoelectric materials with an elliptic hole[J]. *Engineering Mechanics*, 2012, 29(12): 45–50. (in Chinese)

[21] DU Y L, LIU S H, DUAN S J, et al. Electro-elastic fields of piezoelectric materials with an elliptic hole under uniform internal shearing forces[J]. *Chinese Journal of Mechanical Engineering*, 2013, 26(3): 467–474.

[22] LIU S H, QI Y Q, FENG D D, et al. Numerical analysis of a crack emanating from an elliptical hole[J]. *Journal of Mechanical Engineering*, 2012, 48(20): 83–87. (in Chinese)

[23] MIAO C Q, WEI Y T, YAN X Q. Interactions of two collinear circular hole cracks subjected to internal pressure[J]. *Applied Mathematics and Computation*, 2013, 223: 216–224.

## Biographical notes

LIU Shuhong, born in 1968, is currently a professor at *Shijiazhuang Tiedao University, China.* She received her PHD degree from *Beijing Jiaotong University*, *China*, in 2004. Her main research interests include solid mechanics, structural safety evaluation, and mechanical bearing capacity of intelligent materials.
Tel: +86-311-87936546; E-mail: liush@stdu.edu.cn

DUAN Shijie, born in 1968, is currently an associate professor at *Shijiazhuang Tiedao University, China.* He received his bachelor degree from *Shijiazhuang Tiedao University, China,* in 1992. His research interest is computer application in engineering.
Tel: +86-311-87935139; E-mail: dsj1968@sohu.com